Optimal and Reinforced Robustness Designs of Fuzzy Variable Structure Tracking Control for a Piezoelectric Actuator System

Chih-Lyang Hwang and Chau Jan

***Abstract*—In this paper, a piezoelectric actuator (PEA) system is approximated by N subsystems, which are described by pulse transfer functions. The approximation error between the PEA system and the fuzzy linear pulse transfer function system is represented by additive nonlinear time-varying uncertainties in every subsystem. First, a dead-beat to the switching surface for every ideal subsystem is designed. It is called the "variable structure tracking control." The output disturbance of the ith subsystem is caused by the approximation error of fuzzy-model and the interaction dynamics resulting from other subsystems. In general, it is not small. Then, the H^{∞}-norm of the sensitivity function between the switching surface and the output disturbance is minimized. It is the "optimal robustness." Although the effect of the output disturbance is attenuated, a better performance can be reinforced by a switching control which is based on the Lyapunov redesign. This is the final step for the robustness design of control, which is "reinforced robustness." The stability of the overall system is verified by Lyapunov stability theory. Experimental work of a PEA system was carried out to confirm the validity of the proposed control.**

***Index Terms*—Dead-beat control, discrete-time variable structure control, fuzzy linear pulse transfer function (FLPTF), Lyapunov stability theory, piezoelectric actuator (PEA) system, sensitivity minimization in H^{∞}-norm space.**

I. Introduction

PIEZOELECTRICITY is a fundamental process of electromechanical interaction and is representative of coupling in energy conversion. It relates dielectric displacement/electric field to mechanical stress/strain in piezoelectric materials. The application of an electric field to piezoelectric materials can introduce mechanical stress/strain. Also, the position measurement can be obtained by capacitive sensor. It is a well-known commercially available device for managing extremely small displacements in the range from 10 pm to a few 100 μm [1]–[7]. Piezoelectric structures are widely used in applications that require electric to mechanical energy conversion coupled with size limitations, precision and speed of operation, e.g., precision sensors, precision positioners, speakers, shutters, and impact print hammers.

Recently, Tao and Kokotovic [5] use a simplified hysteresis model to reduce the effect of hysteretic nonlinearities. However, the assumptions of minimum phase system and known relative degree must be met. Ge and Jouaneh [6] discuss a comparison between a feedforward control, a regular PID control, and a PID feedback control with hysteresis modeling in the feedforward loop. However, the control methods are dependent on the complex Preisach model and are limited to a sinusoidal trajectory. The nonlinear dynamics of the piezoelectric actuator (PEA) is first linearized and then reformulated into a standard almost disturbance decoupling problem in [7]. However, the result is only suitable for a small operation range. Hwang *et al.* [8] use a forward control to approximately cancel the hysteresis and then apply a discrete variable structure control to enhance the performance. There feedforward control is not required.

In general, fuzzy systems can be classified as Mamdani fuzzy systems and Takagi–Sugeno (T–S) fuzzy systems [9]. Mamdani fuzzy systems use fuzzy sets as rule consequent. However, T–S fuzzy systems use functions of input variables as rule consequent. In many studies (e.g., [10]–[12]), a nonlinear system was first approximated by a T–S fuzzy linear model. Then, a model-based fuzzy control was developed to stabilize the T–S fuzzy linear model. Tanaka *et al.* [10] present fuzzy linear robust control with all state available for a class of uncertain nonlinear systems. For attenuating the effect of unmodeled dynamics, H^{∞} optimization is employed to design a fuzzy linear control for nonlinear dynamic systems [11]. Johansen *et al.* [12] define a multiobjective identification of the dynamic T–S fuzzy model that is a good approximation of both local and global dynamics of the underlying system. However, these objectives are often conflicting. Alternatively, a robust controller is still required to obtain a better system performance. Moreover, the aforementioned approaches [9]–[12] need an observer if the state is not accessible.

In this paper, fuzzy linear models are adopted to approximate the PEA system. The fuzzy models of the proposed control only need the second-order discrete-time input/output models for different operating conditions [i.e., the linear pulse transfer function (LPTF) systems]; they can be easily achieved by the recursive least-squares parameter estimation [13] for different premise variables. The approximation error between the PEA system and the fuzzy LPTF (FLPTF) system is then characterized as the additive nonlinear time-varying uncertainty (ANTVU) in every subsystem. A dead-beat to the switching surface for every ideal subsystem is first designed. It is called the "variable structure tracking control." In the current paper, the output disturbance is caused by the approximation error of fuzzy-model and the interaction dynamics resulting from

Manuscript received April 19, 2002; revised September 10, 2002 and October 4, 2002. This work was supported by the Project of Basic Research of Tatung University under Grant B90-1100-05, and by the National Science Council of Taiwan, R.O.C., under Grant NSC-91-2212-E-036-006.

The authors are with the Department of Mechanical Engineering, Tatung University, Taipei 10451, Taiwan, R.O.C. (e-mail: clhwang@ttu.edu.tw).

Digital Object Identifier 10.1109/TFUZZ.2003.814838

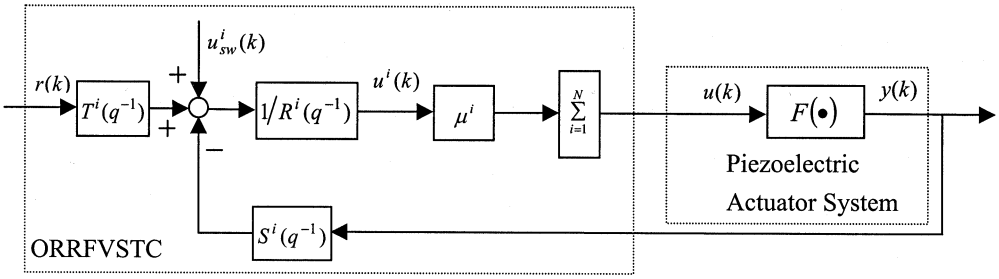

Fig. 1. Control block diagram.

other subsystems. In general, it may not be small. Then, the H^∞-norm of the sensitivity function between the switching surface and the output disturbance is minimized. It is the so-called "optimal robustness." Although the effect of the output disturbance is reduced, a better performance can be reinforced by a switching control which is based on the Lyapunov redesign. This is the final step for the robustness design of control, which is called as "reinforced robustness." In short, the proposed control combines the advantages of fuzzy control or modeling (e.g., FLPTF) and robust control (e.g., dead-beat to switching surface, minimax optimization of sensitivity function, Lyapunov redesign for switching control) to design a simple and effective fuzzy robust controller for a PEA system. The experimental results confirm the validity of the proposed control.

II. Mathematical Preliminaries

A discrete-time signal at the kth sampling interval (i.e., kT) of a continuous signal $x_c(t)$ is represented by $x(k) = x_c(kT) \in \Re$. A polynomial representation is defined as follows: $A(q^{-1}) = a_0 + a_1 q^{-1} + \cdots + a_{n_a} q^{-n_a}$, where a_i, for $i = 0, 1, \ldots, n_a$, denotes bounded real coefficients, n_a is the system degree [i.e., if $a_{n_a} \neq 0$, $\deg\{A(q^{-1})\} = n_a$], and q^{-1} is the backward-time shift operator [i.e., $q^{-1}x(k) \equiv x(k-1)$]. $A_+(q^{-1})$ and $A_-(q^{-1})$ denote the stable and unstable part of $A(q^{-1})$, respectively. Without loss of generality, the polynomial $A_+(q^{-1})$ is assumed to be monic [i.e., $A_+(0) = 1$] to render a unique factorization. The superscript i of a polynomial, e.g., $A^i(q^{-1})$, represents the polynomial of the ith subsystem. The symbol $\overline{A}^i_-(q^{-1}) = q^{-n^i_a} A^i_-(q)$ is used. Then, the rational function $A^i_-(q^{-1})/\overline{A}^i_-(q^{-1})$ is a stable, causal, and all-pass operator, i.e., $\left|A^i_-(e^{-jw})/\overline{A}^i_-(e^{-jw})\right| = 1$. The notation $\left\|A(q^{-1})\right\|_\infty = ess.\sup_{0\le w\le 2\pi}\left|A(e^{-jw})\right|$ is adopted.

M_j denotes a fuzzy set of $z_j(k)$; M^i_j denotes a fuzzy term of M_j selected for *rule i*. $\prod_{j=1}^{N} f_j = f_1 f_2 \cdots f_N$ denotes a scalar multiplication. $\delta(k)$ is the Kronecker delta: $\delta(k) = 1$, if $k = 0$, $\delta(k) = 0$, otherwise.

III. Problem Formulation

Consider the following PEA system (cf. Fig. 1):

$$y(k) = F[y(k-1), \ldots, y(k-n), u(k-1), \ldots, u(k-m)] \quad (1)$$

where $F(\cdot)$ represents an unknown PEA system, $y(k)$ and $u(k)$ denote the system output and the system input, respectively.

A fuzzy dynamic model to represent local linear input/output relations of the PEA system is described by fuzzy IF–THEN rules. The ith rule of this fuzzy dynamic model for the PEA system is expressed as follows:

System Rule i:

$$\begin{aligned}&\text{IF } z_1(k) \text{ is } M^i_1 \cdots \quad \text{and} \quad z_{\overline{n}}(k) \text{ is } M^i_{\overline{n}}\\ &\text{THEN } y(k) = q^{-d^i} B^i(q^{-1})u(k)/A^i(q^{-1})\end{aligned} \quad (2)$$

where $\overline{n} \le n^i_a + n^i_b + 1$, $A^i(0) = 1$, $d^i \ge 1$ is the delay (i.e., $b^i_0 \neq 0$) for $i = 1, 2, \ldots, N$, where N is the number of IF–THEN rules, $y(k)$ denotes the output from the ith IF–THEN rules, and $z_1(k), \ldots, z_{\overline{n}}(k)$ are premise variables which are functions of $y(k-1), \ldots, y(k-n^i_a)$, $u(k-d^i), \ldots, u(k-n^i_b-d^i+1)$. Assume that $A^i(q^{-1})$ and $B^i(q^{-1})$ are coprime, $i = 1, 2, \ldots, N$.

The output of the overall fuzzy system is inferred as follows:

$$y(k) = \sum_{i=1}^{N} \mu^i(k)\left\{q^{-d^i} B^i(q^{-1})u(k) \Big/ A^i(q^{-1})\right\} \quad (3)$$

where $\mu^i(k) = h^i(k)/\sum_{i=1}^{N} h^i(k)$ and $h^i(k) = \prod_{j=1}^{\overline{n}} M^i_j(z(k))$. Based on the approximation of fuzzy linear model (e.g., [9]–[12]), the PEA system is approximated by the overall fuzzy model with the following ANTVU $\Delta^i(u(k-1), k)$ in every subsystem [14]:

$$\begin{aligned}&F[y(k-1), \ldots, y(k-n), u(k-1), \ldots, u(k-m)]\\ &\quad = \sum_{i=1}^{N} \mu^i(k)\left\{q^{-d^i} B^i(q^{-1})u(k) \Big/ A^i(q^{-1})\right.\\ &\qquad\qquad \left. + \Delta^i(u(k-1), k)\right\}\end{aligned} \quad (4)$$

where $\left|\Delta^i(u(k-1), k)\right| \le \alpha^i_1 |u(k-1)| + \alpha^i_2$, $\forall k$, i, and α^i_1, α^i_2 are bounded. The ANTVU $\Delta^i(u(k-1), k)$ is caused by the hysteretic feature of the PEA system. Assume that the fuzzy controller shares the same fuzzy sets with the fuzzy system (2)

Control Rule i:

$$\begin{aligned}&\text{IF } z_1(k) \text{ is } M^i_1 \cdots \quad \text{and} \quad z_{\overline{n}}(k) is M^i_{\overline{n}}\\ &\text{THEN } u(k) = \left\{-S^i(q^{-1})y(k) + T^i(q^{-1})r(k) + u^i_{sw}(k)\right\}\\ &\qquad\qquad \Big/ R^i(q^{-1})\end{aligned} \quad (5)$$

where the polynomials $R^i(q^{-1})$, $S^i(q^{-1})$ and $T^i(q^{-1})$ are selected such that the ith subsystem (2) is stable and the specific trajectory tracking is accomplished, and $u^i_{sw}(k)$ represents the

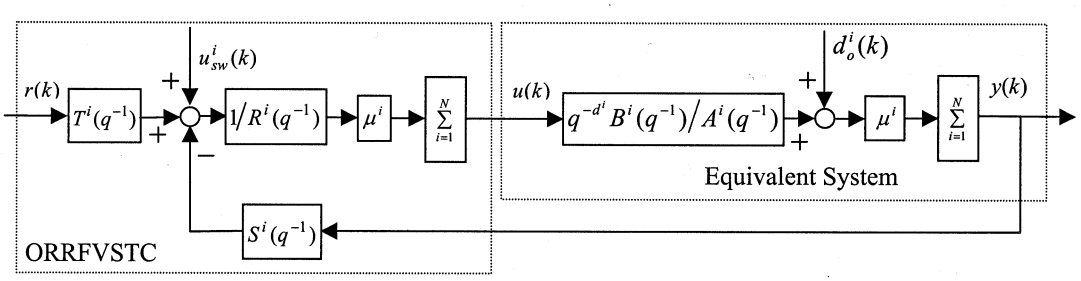

Fig. 2. Equivalent control block diagram of Fig. 1.

switching control of the ith subsystem (2) to improve the system performance. The overall fuzzy control is inferred as follows:

$$u(k)=\sum_{i=1}^{N}\mu^i(k)\left\{\left[-S^i(q^{-1})y(k)+T^i(q^{-1})r(k)+u^i_{sw}(k)\right]/R^i(q^{-1})\right\}. \quad (6)$$

The nominal closed-loop characteristic polynomial of the ith subsystem is defined as follows:

$$A^i_c(q^{-1})=A^i(q^{-1})R^i(q^{-1})+q^{-d^i}B^i(q^{-1})S^i(q^{-1}). \quad (7)$$

Then, the closed-loop output response of the ith subsystem is obtained from (4) and (6)

$$y(k)=\sum_{i=1}^{N}\mu^i(k)\left\{\left[q^{-d^i}B^i(q^{-1})\Big/\left(A^i(q^{-1})R^i(q^{-1})\right)\right]\cdot\left[-S^i(q^{-1})y(k)+T^i(q^{-1})r(k)+u^i_{sw}(k)\right]+\Delta^i(u(k-1),k)+\phi^i(k)\right\} \quad (8)$$

where $\phi^i(k)=q^{-d^i}B^i(q^{-1})[u(k)-u^i(k)]/A^i(q^{-1})$, where $u^i(k)$ is the same as (5), denotes an interaction dynamics on the ith subsystem due to other subsystems. After some mathematical manipulations, we have

$$\sum_{i=1}^{N}\frac{\mu^i(k)A^i_c(q^{-1})}{A^i(q^{-1})R^i(q^{-1})}\left\{y(k)-\frac{q^{-d^i}B^i(q^{-1})T^i(q^{-1})}{A^i_c(q^{-1})}r(k)-\frac{q^{-d^i}B^i(q^{-1})}{A^i_c(q^{-1})}u^i_{sw}(k)-\frac{A^i(q^{-1})R^i(q^{-1})}{A^i_c(q^{-1})}d^i_o(k)\right\}=0 \quad (9)$$

where $d^i_o(k)=\Delta^i(u(k-1),k)+\phi^i(k)$ denotes the output disturbance of the ith subsystem caused by the approximation of fuzzy-model and the interaction dynamics. It may not be small. Hence, a sufficient condition for the existence of (9) is the term in braces $\{\cdot\}$ of (9) is equal to zero, i.e.,

$$y(k)=\left\{q^{-d^i}B^i(q^{-1})T^i(q^{-1})r(k)+q^{-d^i}B^i(q^{-1})u^i_{sw}(k)+A^i(q^{-1})R^i(q^{-1})d^i_o(k)\right\}\Big/A^i_c(q^{-1}). \quad (10)$$

This is the output of the ith closed-loop subsystem. The reference input is assumed as follows:

$$r(k)=G_r(q^{-1})\delta(k)/F_r(q^{-1}) \quad (11)$$

where $G_r(q^{-1})$ and $F_r(q^{-1})$ are coprime. Define the following switching surface:

$$\sigma(k)=C(q^{-1})e(k) \quad (12)$$

where $e(k)=r(k)-y(k)$ and $C(q^{-1})$ is a stable monic polynomial. Then, the switching surface response $\sigma(k)$ from the inputs $r(k)$, $d^i_o(k)$ and $u^i_{sw}(k)$ is accomplished from (12) and (8), i.e.,

$$\sigma(k)=\sum_{i=1}^{N}\mu^i(k)\left\{P^i(q^{-1})r(k)-V^i(q^{-1})d^i_o(k)-W^i(q^{-1})u^i_{sw}(k)\right\} \quad (13a)$$

where

$$P^i(q^{-1})=C(q^{-1})\left[A^i_c(q^{-1})-q^{-d^i}B^i(q^{-1})T^i(q^{-1})\right]\Big/A^i_c(q^{-1}) \quad (13b)$$

$$V^i(q^{-1})=C(q^{-1})A^i(q^{-1})R^i(q^{-1})/A^i_c(q^{-1}) \quad (13c)$$

$$W^i(q^{-1})=q^{-d^i}C(q^{-1})B^i(q^{-1})/A^i_c(q^{-1}). \quad (13d)$$

The major contributions of this paper are described as follows (cf. Figs. 1 and 2).

1) A fuzzy control based on a FLPTF [i.e., (2)] is constructed to stabilize the PEA system (1) or (4) subject to the output disturbance of the ith subsystem [i.e., $d^i_o(k)$].
2) The fuzzy equivalent control [i.e., the polynomials $R^i(q^{-1})$, $S^i(q^{-1})$ and $T^i(q^{-1})$] is designed to satisfy the following two requirements.
   a) For the ideal subsystem [i.e., $d^i_o(k)=u^i_{sw}(k)=0$], the response of the operating point is dead-beat to the switching surface [13].
   b) A minimax optimization for sensitivity function [i.e., minimization of $\left\|V^i(q^{-1})\right\|_\infty$] is employed to attenuate the effect of the output disturbance.
3) Based on the Lyapunov redesign, the switching control of ith subsystem [i.e., $u^i_{sw}(k)$] is then designed to reinforce the performance of the PEA system (1).
4) The corresponding experiments are arranged to verify the validity of the proposed control. It is not limited to sinusoidal trajectories.

IV. Fuzzy Modeling of Piezoelectric Actuator System

The dynamics of the PEA system is strongly dependent on the hysteresis behavior [8]. The dominant factors of the hysteretic loop are the magnitude and the polarity of the input signal (cf. Fig. 3). The frequency of the input signal mildly influences the

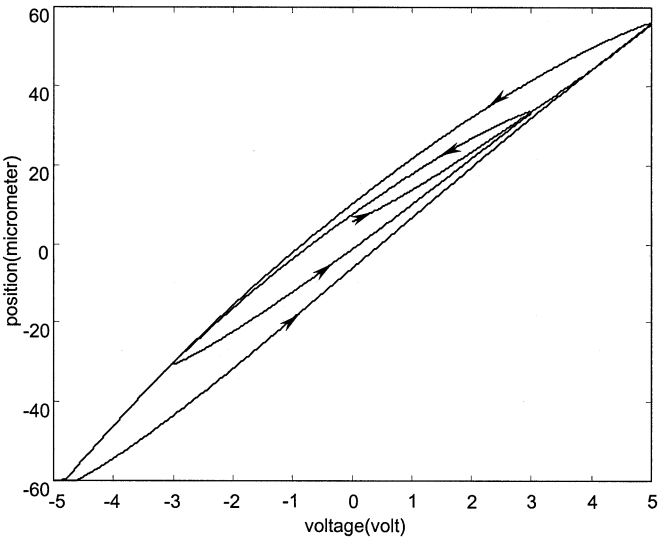

Fig. 3. Hysteresis characteristic.

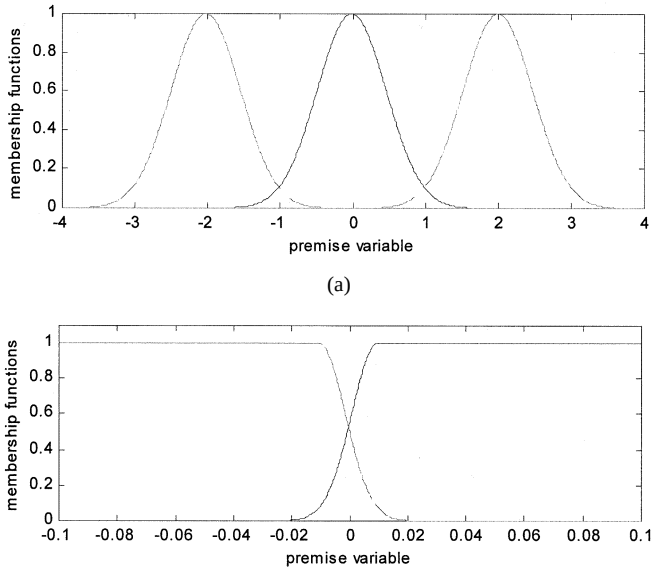

Fig. 4. Experimental setup of the overall system. (a) Photograph. (b) Control block diagram.

dynamics of PEA. Hence, the premise variables are defined as follows: $z_1(k) = u(k-1)$ and $z_2(k) = u(k-1) - u(k-2)$ (see Fig. 4). Consequently, the number and distribution of membership functions are suitably determined. A system input (e.g., a combination of different magnitudes and frequencies of sinusoidal signal or only one fixed frequency of sinusoidal signal) is applied to the PEA system. Thus the input/output data corresponding to the ith fuzzy rule (or subsystem) are fed into the following recursive least squares parameter estimation (14) (e.g., [13]) to obtain the coefficients of the polynomials $A^i(q^{-1})$ and $B^i(q^{-1})$

$$\hat{\theta}^i(k) = \hat{\theta}^i(k-1) + \Gamma^i(k)[y(k) - \Phi^i(k)^T\hat{\theta}^i(k-1)] \quad (14a)$$

$$\Gamma^i(k) = P^i(k-1)\Phi^i(k)/[1 + \Phi^i(k)^T P^i(k-1)\Phi^i(k)] \quad (14b)$$

$$P^i(k) = P^i(k-1) - \Gamma^i(k)\Pi^i(k)^T P^i(k-1) \quad (14c)$$

where

$$\hat{\theta}^i(k) = [\,\hat{a}^i_1(k) \quad \cdots \quad \hat{a}^i_{n_a}(k) \quad \hat{b}^i_0(k) \quad \cdots \quad \hat{b}^i_{n_b}(k)\,]^T \quad (14d)$$

$$\Phi^i(k) = [\,-y(k-1) \quad -y(k-n^i_a) \quad u(k-d^i) \quad u(k-d^i+1-n^i_b)\,]^T. \quad (14e)$$

The initial values $\hat{\theta}^i(0)$ and $P^i(0) = \kappa I$ for $i = 1, 2, \ldots, N$ (I is an unit matrix and κ is a sufficiently large positive real number) are set. Similarly, other subsystems are obtained. Due to the advantage of the fuzzy-model, the linear dynamic models obtained from the input/output data by (14) are easy and acceptable. Finally, all the subsystems are combined together by the normalized weighting $\mu^i(k)$, for $i = 1, 2, \ldots, N$ to form a fuzzy-model of the PEA system. The details are in Section VI.

After the achievement of the fuzzy-model for the PEA system, a verification of fuzzy-model (e.g., sinusoidal responses of different frequencies and magnitudes for the fuzzy-model and the PEA system) must be arranged to confirm the effectiveness of the proposed modeling. If the fuzzy-model is not acceptable for representing the PEA system, the following modifications are made to enhance the fuzzy modeling of PEA system.

1) *An adjustment of the shape of membership function* is first proposed to enhance the accuracy of modeling.
2) If the modeling is still not satisfactory, *an increase of the fuzzy rule* is arranged to enhance the performance of modeling.
3) *A different selection of the premise variables* is also suggested to improve the accuracy of modeling.
4) *An optimization procedure based on some input/output data* is applied to obtain a more effective fuzzy-model.

V. Controller Design

A. Dead-Beat to Switching Surface of the ith Subsystem

First, the output disturbance and the switching control are assumed to be zero. For achieving the dead-beat (or finite-time arrival) of the switching surface, the overall response of the switching surface $\sigma(k)$ must have the following form:

$$\sigma(k) = \sum_{i=1}^{N} \mu^i(k)\sigma^i(k) = \sum_{i=1}^{N} \mu^i(k)H^i(q^{-1})\delta(k) \quad (15)$$

where $H^i(q^{-1})$ is a polynomial of ith subsystem with the degree which is the same as the number of dead-beat steps [15].

Remark 1: Because $\sum_{i=1}^{N} \mu^i(k) = 1$, $\sigma^i(k) = \sigma(k)$ if $\sigma^i(k)$ is same for every subsystem. In addition, the polynomial $C(q^{-1})$ in (12) is assumed to be the same for every subsystem.

Substituting (11) and (13b) into (13a) gives

$$\sigma(k) = \sum_{i=1}^{N} \mu^i(k)\Big\{C(q^{-1})\Big[A^i_c(q^{-1}) - q^{-d^i}B^i(q^{-1})T^i(q^{-1})\Big] \cdot G_r(q^{-1})\delta(k)\Big/\left[A^i_c(q^{-1})F_r(q^{-1})\right]\Big\}. \quad (16)$$

Comparing (15) and (16) yields

$$\frac{T^i(q^{-1})}{A^i_c(q^{-1})} = \frac{G_r(q^{-1})C(q^{-1}) - F_r(q^{-1})H^i(q^{-1})}{q^{-d^i}B^i(q^{-1})G_r(q^{-1})C(q^{-1})}. \quad (17)$$

Since $A_c^i(q^{-1})$ is stable, the denominator of the right-hand side of (17) must be stable. Hence, the following equations are obtained:

$$H^i(q^{-1}) = L^i(q^{-1})G_{r\_}(q^{-1}) \tag{18}$$

$$G_{r_+}(q^{-1})C(q^{-1}) - F_r(q^{-1})L^i(q^{-1}) = q^{-d^i}B_{\_}^i(q^{-1})\Gamma^i(q^{-1}). \tag{19}$$

Rewrite (19) as the following Diophantine equation:

$$F_r(q^{-1})L^i(q^{-1}) + q^{-d^i}B_{\_}^i(q^{-1})\Gamma^i(q^{-1}) = G_{r_+}(q^{-1})C(q^{-1}) \tag{20}$$

where $F_r(q^{-1})$ and $q^{-d^i}B_{\_}^i(q^{-1})$ are coprime, the monic polynomial $L^i(q^{-1})$ with the degree $n_l^i = n_{b\_}^i + d^i - 1$, and the polynomial $\Gamma^i(q^{-1})$ has the degree $n_\gamma^i = n_{f_r}^i - 1$. Assume that

$$R^i(q^{-1}) = \hat{R}^i(q^{-1})B_+^i(q^{-1}). \tag{21}$$

From (7) and (17)–(21), the following equations hold:

$$\begin{aligned} &A^i(q^{-1})\hat{R}^i(q^{-1}) + q^{-d^i}B_{\_}^i(q^{-1})S^i(q^{-1}) \\ &\quad = C(q^{-1})G_{r_+}(q^{-1})X^i(q^{-1}) \end{aligned} \tag{22}$$

$$T^i(q^{-1}) = \Gamma^i(q^{-1})X^i(q^{-1}) \tag{23}$$

where $X^i(q^{-1})$ is a stable polynomial with the degree $n_x^i = n_a^i + n_{b\_}^i + d^i - n_{g_{r+}} - n_c - 1$. From (20), (21), (22) and (7), the following nominal closed-loop characteristic polynomial is then obtained:

$$A_c^i(q^{-1}) = C(q^{-1})G_{r_+}(q^{-1})B_+^i(q^{-1})X^i(q^{-1}). \tag{24}$$

The previous design addresses the finite-time setting to the switching surface for the ideal ith subsystem.

B. Minimax Optimization of Sensitivity Function

In this subsection, the task is to find the polynomials $R^i(q^{-1})$ and $S^i(q^{-1})$ such that the minimization of $\left\|V^i(q^{-1})\right\|_\infty$ is simultaneously achieved. Based on the previous results, the minimization must satisfy the following interpolation constraints [14], [16], [17]:

$$V^i(p_j^i) = 0, \qquad j = 1, 2, \ldots, n_{a\_}^i \tag{25a}$$

$$1 - V^i(z_j^i)/C(z_j^i) = 0, \qquad j = 1, 2, \ldots, n_z^i - 1 \tag{25b}$$

where $n_z^i = d^i + n_{b\_}^i$, $p_j^i (1 \le j \le n_{a\_}^i)$ and $z_j^i (1 \le j \le n_z^i - 1)$ denote the zeros of $A_{\_}^i(q^{-1})$ and $q^{-d^i}B_{\_}^i(q^{-1})$, respectively.

Lemma 1 [14], [16], [17]:

1) The optimal $V^i(q^{-1})^*$ which minimizes $\left\|V^i(q^{-1})\right\|_\infty$ is of an all-pass form

$$V^i(q^{-1})^* = \begin{cases} \rho^i \overline{\Psi}^i(q^{-1}) / \Psi^i(q^{-1}), & \text{if } n_z^i = n_\psi^i + 1 \ge 1 \\ 0, & \text{if } n_z^i = 0 \end{cases}$$

where the polynomial $\Psi^i(q^{-1})$ is monic and stable.

2) The constant ρ^i and $\psi_j^i (1 \le i \le N, 1 \le j \le n_\psi^i)$ are real and are uniquely determined by the interpolation constraints (25). Furthermore, the minimized $\left\|V^i(q^{-1})\right\|_\infty$ is given by

$$\min \left\|V^i(q^{-1})\right\|_\infty = \left\|V^i(q^{-1})^*\right\|_\infty = \left|\rho^i\right|.$$

Based on the result of *Lemma 1* and the constraint (25), the following equation is achieved:

$$V^i(q^{-1}) = \rho^i A_{\_}^i(q^{-1})\overline{\Psi}^i(q^{-1}) \big/ \left[\overline{A}^i{}_{\_}^i(q^{-1})\Psi^i(q^{-1})\right]. \tag{26}$$

Furthermore, the constraint (25b) yields the following result:

$$\begin{aligned} C(q^{-1})\overline{A}^i{}_{\_}^i(q^{-1})\Psi^i(q^{-1}) - \rho^i A_{\_}^i(q^{-1})\overline{\Psi}^i(q^{-1}) \\ = q^{-d^i}B_{\_}^i(q^{-1})M^i(q^{-1}) \end{aligned} \tag{27}$$

where $n_\psi^i = d^i + n_{b\_}^i - 1$ and $n_m^i = n_c + n_{a\_}^i - 1$. This, in turn, means

$$C(z_j^i)\overline{A}^i{}_{\_}^i(z_j^i)\Psi^i(z_j^i) - \rho^i A_{\_}^i(z_j^i)\overline{\Psi}^i(z_j^i) = 0. \tag{28}$$

By the solution of (28) for ρ^i and $\Psi^i(q^{-1})$, the following equations are obtained from (13c) and (26):

$$A_c^i(q^{-1}) = C(q^{-1})A_+^i(q^{-1})\overline{A}^i{}_{\_}^i(q^{-1})\Psi^i(q^{-1})\tilde{X}^i(q^{-1}) \tag{29}$$

$$R^i(q^{-1}) = \rho^i \overline{\Psi}^i(q^{-1})\tilde{X}^i(q^{-1}). \tag{30}$$

Comparing (29) and (24) results in

$$\begin{aligned} \tilde{X}^i(q^{-1}) &= G_{r+}(q^{-1})B_+^i(q^{-1})\hat{X}^i(q^{-1}) \\ X^i(q^{-1}) &= A_+^i(q^{-1})\overline{A}^i{}_{\_}^i(q^{-1})\Psi^i(q^{-1})\hat{X}^i(q^{-1}) \end{aligned} \tag{31}$$

where $\hat{X}^i(q^{-1})$ is a stable polynomial. Then, from (29)–(31)

$$\begin{aligned} A_c^i(q^{-1}) &= C(q^{-1})A_+^i(q^{-1})\overline{A}^i{}_{\_}^i(q^{-1})\Psi^i(q^{-1}) \\ &\quad \cdot G_{r+}^i(q^{-1})B_+^i(q^{-1})\hat{X}^i(q^{-1}) \end{aligned} \tag{32}$$

$$R^i(q^{-1}) = \rho^i \overline{\Psi}^i(q^{-1})G_{r_+}(q^{-1})B_+^i(q^{-1})\hat{X}^i(q^{-1}). \tag{33}$$

Using the relations (32), (33), and (27) into (7) yields

$$S^i(q^{-1}) = G_{r_+}(q^{-1})A_+^i(q^{-1})M^i(q^{-1})\hat{X}^i(q^{-1}). \tag{34}$$

From (23) and (31), the polynomial $T^i(q^{-1})$ is achieved as follows:

$$T^i(q^{-1}) = \Gamma^i(q^{-1})A_+^i(q^{-1})\overline{A}^i{}_{\_}^i(q^{-1})\Psi^i(q^{-1})\hat{X}^i(q^{-1}). \tag{35}$$

That is, the control parameters $\left\{R^i(q^{-1}), S^i(q^{-1}), T^i(q^{-1})\right\}$ for the dead-beat to the switching surface and the minimax optimization of the output disturbance are obtained from (33)–(35).

C. Fuzzy Switching Control for Reinforced Robustness

The proposed fuzzy switching control is designed as follows:

$$\begin{aligned} u_{sw}^i(k) = -A_c^i(q^{-1}) &\left\{\sigma(k) + \beta^i(q^{-1})v_{sw}^i(k)\right\} \\ &\big/ \left\{B_+^i(q^{-1})C(q^{-1})\overline{B}^i{}_{\_}^i(q^{-1})\right\} \end{aligned} \tag{36}$$

where $A_c^i(q^{-1})$ is the same as (32), $\beta^i(q^{-1})$ is a causal stable rational weighting function and $v_{sw}^i(k)$ is given in (45). Substituting (36), (13c), and (15) into (13a), we have

$$\begin{aligned} \sigma(k) = \sum_{i=1}^N \mu^i(k) &\left\{H^i(q^{-1})\delta(k) + V^i(q^{-1})^* d_o^i(k) \right. \\ &+ B_{\_}^i(q^{-1})\sigma(k - d^i)/\overline{B}^i{}_{\_}^i(q^{-1}) \\ &\left. + \eta^i(q^{-1})v_{sw}^i(k - d^i)\right\} \end{aligned} \tag{37}$$

where $\eta^i(q^{-1}) = \beta^i(q^{-1})B_{\_}^i(q^{-1})/\overline{B}^i{}_{\_}^i(q^{-1})$. The results of the first and second terms in the left-hand side of (37) are obtained from Sections V-A and V-B, respectively. By a

suitable selection of the weighting function $\beta^i(q^{-1})$, $\eta^i(q^{-1})$ is designed as a low-pass filter to attenuate the high-frequency component of switching control of the ith subsystem [18]. Based on the facts in (4) and $d_o^i(k) = \Delta^i(u(k-1), k) + \phi^i(k)$, the signal $V^i(q^{-1})^*\Delta^i(u(k-1), k)$ in (37) contains the effect of the switching control of the ith subsystem, i.e., $v_{sw}^i(k-d^i)$. It must be decomposed into two parts for the stability analysis: one includes $v_{sw}^i(k-d^i)$ and the other is without it. From (4), (6), and (12), the following equation is assume to be true:

$$V^i(q^{-1})^*\Delta^i(u(k-1), k) = \gamma_1^i(k)v_{sw}^i(k-d^i) + \gamma_2^i(k)\sigma(k-d^i) + \gamma_3^i(k) \quad (38)$$

where $\left|\gamma_1^i(k)\right| < k_1 < 1$, $\left|\gamma_2^i(k)\right| < k_2$, $\left|\gamma_3^i(k)\right| < k_3$, $\forall k, i$. However, the interaction dynamics $\phi^i(k)$ does not contain $v_{sw}^i(k-d^i)$. Define the difference of $\sigma^i(k)$ as follows:

$$\Delta\sigma^i(k) = \sigma^i(k+d^i) - \sigma^i(k). \quad (39)$$

Thus, from (36) and (39)

$$\Delta\sigma(k) = \sum_{i=1}^{N} \mu^i(k)\Delta\sigma^i(k) = \sum_{i=1}^{N} \mu^i(k)\left\{\Lambda^i(k) + \left[1 - \tau^i(q^{-1}, k)\right] v_{sw}^i(k)\right\} \quad (40)$$

where

$$\tau^i(q^{-1}, k) = 1 - \eta^i(q^{-1}) - \gamma_1^i(k) \quad (41)$$

$$\Lambda^i(k) = H^i(q^{-1})\delta(k+d^i) + V^i(q^{-1})^*\phi^i(k+d^i) + \left\{\gamma_2^i(k+d^i) + \left[B_-^i(q^{-1}) - \overline{B}_-^i(q^{-1})\right] \Big/ \overline{B}_-^i(q^{-1})\right\}\sigma(k) + \gamma_3^i(k+d^i). \quad (42)$$

The upper bound of $\Lambda^i(k)$ is estimated as follows:

$$\left\|\Lambda^i(k)\right\| \le g_\lambda^i(k) = \lambda_0^i\left|\sigma(k)\right| + \lambda_1^i \quad (43)$$

where $\lambda_1^i \ge 0$, $\left[(1-\overline{\lambda}^i)^2 - \varepsilon^i(1+\overline{\lambda}^i)^2\right] / \left[4(1+\overline{\lambda}^i)\right] > \lambda_0^i \ge 0, 1 > (1-\overline{\lambda}^i)^2/(1+\overline{\lambda}^i)^2 > \varepsilon^i > 0, 1 > \overline{\lambda}^i = k_1 + \upsilon^i$, satisfying the following inequality:

$$\left\|1 - \eta^i(q^{-1})\right\|_\infty \le \upsilon^i < 1 \qquad \text{on } D^i \quad (44)$$

where $D^i = \{q \in C \| |q| < 1\}$ is the domain containing the poles of $\beta^i(q^{-1})$ and the zeros of $\overline{B}_-^i(q^{-1})$. The control in (45) is then employed to deal with the unmodeled dynamics $\Lambda^i(k)$

$$v_{sw}^i(k) = \begin{cases} -\xi^i(k)g_\lambda^i(k)\sigma(k) \Big/ \left[(1-\overline{\lambda}^i)(1+\overline{\lambda}^i)\left|\sigma(k)\right|\right], \\ \qquad \text{if } \left|\sigma(k)\right| > \chi^i(k) \\ 0, \qquad \text{otherwise} \end{cases} \quad (45)$$

where

$$\chi^i(k) = \max\left\{4(1+\overline{\lambda}^i)\lambda_1^i \Big/ \left[(1-\overline{\lambda}^i)^2 - \varepsilon^i(1+\overline{\lambda}^i)^2 - 4(1+\overline{\lambda}^i)\lambda_0^i\right] 4(1+\overline{\lambda}^i)g_\lambda^i(k) \Big/ \left[(1-\overline{\lambda}^i)^2 - \varepsilon^i(1+\overline{\lambda}^i)^2\right]\right\}. \quad (46)$$

The switching gain in (45) satisfies the following inequality:

$$\xi_2^i(k) > \xi^i(k) > \xi_1^i(k) \ge 0 \quad (47a)$$

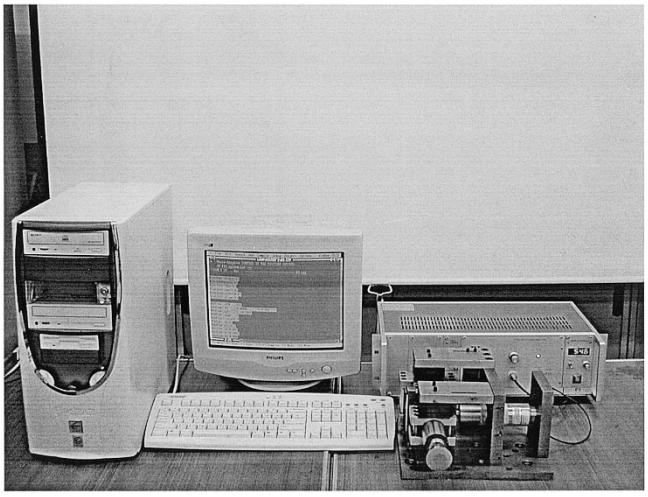

(a)

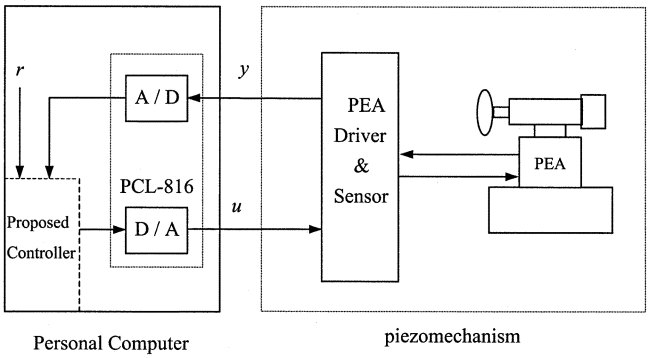

(b)

Fig. 5. Membership functions for premise variables. (a) $z_1(k)$. (b) $z_2(k)$.

where

$$\xi_{1,2}^i(k) = g_1^i(k) \pm \sqrt{\left[g_1^i(k)\right]^2 - g_2^i(k)} \quad (47b)$$

$$g_1^i(k) = (1-\overline{\lambda}^i)^2\left|\sigma(k)\right| / \left[(1+\overline{\lambda}^i)g_\lambda^i(k)\right] - (1-\overline{\lambda}^i) \quad (47c)$$

$$g_2^i(k) = (1-\overline{\lambda}^i)^2\left\{\left[g_\lambda^i(k)\right]^2 + 2g_\lambda^i(k)\left|\sigma(k)\right| + \varepsilon^i\left|\sigma(k)\right|^2\right\} \Big/ \left[g_\lambda^i(k)\right]^2. \quad (47d)$$

Theorem 1: Consider the system (1) and the controller (7) with $u_{sw}^i(k)$ in (36) and $v_{sw}^i(k)$ in (45). Suppose the polynomials $R^i(q^{-1})$, $S^i(q^{-1})$ and $T^i(q^{-1})$ are achieved from (33)–(35). Suppose also that the inequalities in (43) and (44) are satisfied. Then, $\{u(k)\}$ is bounded, $\{\sigma(k)\}$ is bounded in the sense of the minimum sensitivity between the switching surface and the output disturbance, and

$$D_\sigma = \left\{\sigma(k):\ \left|\sigma(k)\right| \le \sum_{i=1}^{N} \mu^i(k)\chi^i(k)\right\}. \quad (48)$$

Proof: See the Appendix.

D. Proposed Control Algorithm

The proposed design procedure for the control algorithm is described as follows.

Step 1) Factorize the ith subsystem as $A^i(q^{-1}) = A_+^i(q^{-1})A_-^i(q^{-1})$, $B^i(q^{-1}) = B_+^i(q^{-1})B_-^i(q^{-1})$.

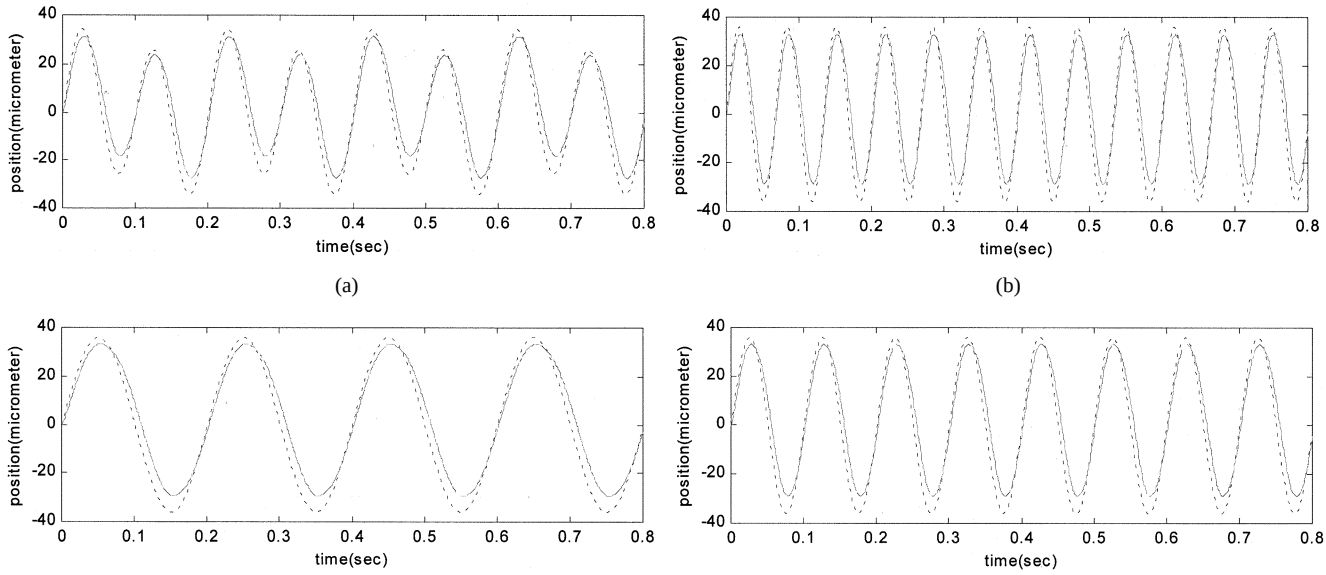

Fig. 6. The output responses of system $(-)$ for the inputs $(\cdots)$. (a) $6\sin(10\pi k) + 30\sin(20\pi k)$ μm. (b) $36\sin(30\pi k)$ μm. (c) $36\sin(10\pi k)$ μm. (d) $36\sin(20\pi k)$ μm.

Assign a reference input: $G_r(q^{-1})$, $F_r(q^{-1})$; similarly, $G_r(q^{-1}) = G_{r+}(q^{-1})G_{r-}(q^{-1})$. The coefficients of the switching surface in (12) [i.e., $C(q^{-1})$] are also appropriately selected.

Step 2) The polynomials $L^i(q^{-1})$ and $\Gamma^i(q^{-1})$ are obtained from (20). The scalar ρ^i and the polynomial $\Psi^i(q^{-1})$ are from (28); by long division, the polynomial $M^i(q^{-1})$ is then obtained from (27).

Step 3) The equivalent control of the ith subsystem, i.e., $R^i(q^{-1})$, $S^i(q^{-1})$, $T^i(q^{-1})$, for the dead-beat to the switching surface, and the minimax optimization of the output disturbance, are accomplished from (33)–(35) for a stable polynomial $\hat{X}^i(q^{-1})$.

Step 4) The switching control of the ith subsystem is determined from (36) and (45).

Step 5) Finally, the overall fuzzy control is achieved from (6).

VI. Experiments

A. Experimental Setup

The PEA system consists of two parts: piezomechanism (including translator, position sensor, driver, and carriage mechanism) and personal computer [including 16-bit AD/DA card (PCL-816) and proposed control program]. The block diagram of the experimental setup is shown in Fig. 5. The carriage mechanism is made of steel for enhancing the strength of the mechanism. Four linear guides provided by THK Co., Japan (Model no. VRU3088) are used to support the moving part of the mechanism. Furthermore, a high-speed spindle with weight 3.5 kg is fixed on the carriage mechanism. The piezoelectric actuator system is a Model no. P-246.70 from Physical Instrument (PI) Co., Germany. Its specifications are briefly described as follows: maximum expansion 120 μm, electric capacitance 3000 nF, stiffness 190 N/μm, resonant frequency 3.5 kHz, and temperature expansion 2 μm K°. The position signal $y(k)$ is achieved by a position sensor, i.e., Model no. P-177.10 of PI Co. The signal is received by a A/D card in an 80 586 personal computer. Together with a reference input in the computer program written by Turbo C, the control signal $u(k)$ is calculated. The control input through the D/A card is then sent to the driver, which is a Model no. of P-271.10 from PI Co. The output signal of the driver with voltage between -200 and 1000 volt is used to drive the piezoelectric actuator. The different position signal is accomplished by using a different input signal. The process is repeated until the total process time is over. The time required for every process is called the "control cycle time (T_c)." In this paper, $T_c = 0.0008$ s.

TABLE I
Maximum Steady-State Tracking Errors

System type / Reference input	Open-loop system	System using fuzzy equivalent control	System using proposed control
$6\sin(10\pi k)+30\sin(20\pi k)$ μm	8.1 μm	3.2 μm	1.5 μm
$36\sin(10\pi k)$ μm (5Hz)	7.5 μm	3.3 μm	1.7 μm
$36\sin(20\pi k)$ μm (10Hz)	8.5 μm	3.2 μm	1.6 μm
$36\sin(30\pi k)$ μm (15Hz)	9.6 μm	3.5 μm	2.3 μm

The responses of the open-loop PEA system for the inputs: $6\sin(10\pi k) + 30\sin(20\pi k)$ μm, $36\sin(30\pi k)$ μm, $36\sin(10\pi k)$ μm, and $36\sin(20\pi k)$ μm, are presented in the Fig. 6(a)–(d), respectively. The maximum steady-state tracking error of Fig. 6 is about 23.2% of the amplitude of input (cf. its absolute values in Table I). Hence, an effective controller is required.

In addition, the PID controller is employed to control the PEA system. The form of the discrete-time PID controller is described as follows (cf. [6]):

$$u(k) = K_p e(k) + K_p \frac{T_c}{T_I} \sum e(k) + K_p \frac{T_D}{T_c} [e(k) - e(k-1)]. \quad (49)$$

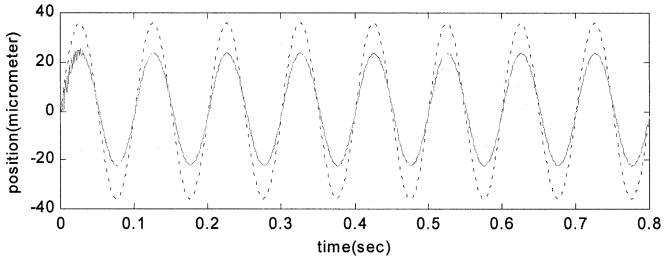

(a)

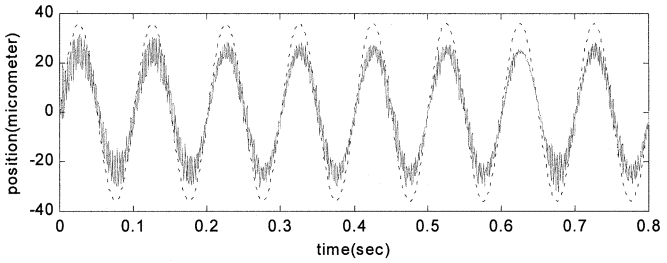

(b)

Fig. 7. The output response of the PID control $(-)$ for the reference input $36\sin(20\pi k)$ μm $(\cdots)$. (a) $T_I = 20$, $T_D = 0.000\,05$, $K_p = 2.2$. (b) $T_I = 20$, $T_D = 0.000\,05$, $K_p = 2.4$.

The responses due to the PID control with $T_I = 20$, $T_D = 0.000\,05$ for the reference input $36\sin(20\pi k)$ μm, and different K_p are depicted in Fig. 7(a) $K_p = 2.2$ and (b) $K_p = 2.4$, respectively. In general, the larger the parameter K_p is, the more accurate the result is. However, in Fig. 7(b) a too large parameter K_p results in an oscillatory response. The other selections of control parameters for (49) render similar response in Fig. 7. Because the PEA fundamentally exhibits the nonlinearity and hysteresis, the linear PID controller cannot have a satisfactory trajectory tracking for the PEA system.

B. Modeling

Based on the result of Section IV, six fuzzy-model rules with the corresponding premise variables $z_1(k)$ and $z_2(k)$ are expressed as follows:

$$\begin{aligned}&\textit{System Rule } i\text{:}\\&\text{IF } z_1(k) \text{ is } M_1^i,\ z_2(k) \text{ is } M_2^i\\&\text{THEN } y(k)=q^{-d^i}B^i(q^{-1})u(k)/A^i(q^{-1}), \qquad i=1,\,2,\,\ldots,\,6\end{aligned} \tag{50}$$

where $d^i = 1, \forall\, i = 1, 2, \ldots, 6$, the membership functions are chosen as follows (cf. Fig. 5):

$$\begin{aligned}&M_1^1(z_1)=e^{-2z_1^2(k)} \quad M_1^2(z_1)=e^{-2(z_1(k)-2)^2}\\&M_1^3(z_1)=e^{-2(z_1(k)+2)^2}\\&M_2^1(z_2)=\begin{cases}e^{-80(z_2(k)-0.01)^2}, & \text{if } z_2(k)\le 0.01\\ 1, & \text{otherwise}\end{cases}\\&M_2^2(z_2)=\begin{cases}e^{-80(z_2(k)+0.01)^2}, & \text{if } z_2(k)\ge -0.01\\ 1, & \text{otherwise.}\end{cases}\end{aligned} \tag{51}$$

The normalizing weight for the fuzzy rule is described as follows: $\mu^i(k) = h^i(k)/\sum_{i=1}^{6} h^i(k)$, where

$$\begin{aligned}&h^1(k)=M_1^1(z_1)\times M_2^1(z_2) \quad h^2(k)=M_1^2(z_1)\times M_2^1(z_2)\\&h^3(k)=M_1^3(z_1)\times M_2^1(z_2) \quad h^4(k)=M_1^1(z_1)\times M_2^2(z_2)\\&h^5(k)=M_1^2(z_1)\times M_2^2(z_2) \quad h^6(k)=M_1^3(z_1)\times M_2^2(z_2).\end{aligned}$$

The nominal coefficients of six subsystems for the input signal $6\sin(10\pi k)+30\sin(20\pi k)$ μm, are presented as follows:

$$\begin{aligned}a_1^{1\sim 6}=&-0.243\,118,\ -0.194\,321,\ -0.198\,19\\&-0.230\,833,\ -0.215\,404,\ -0.212\,554\\a_2^{1\sim 6}=&-0.175\,277,\ -0.255\,805,\ -0.283\,489\\&-0.280\,044,\ -0.253\,760,\ -0.241\,822\\b_0^{1\sim 6}=&\,0.080\,283,\ 0.080\,980,\ 0.074\,071\\&\,0.067\,842,\ 0.060\,033,\ 0.060\,953\\b_1^{1\sim 6}=&\,0.296\,39,\ 0.374\,155,\ 0.441\,181\\&\,0.252\,187,\ 0.363\,276,\ 0.425\,842.\end{aligned} \tag{52}$$

Six subsystems of (52) are all of nonminimum phase and are stable.

The output responses of the mathematical model and the PEA system for the same inputs of Fig. 6, are shown in Fig. 8(a)–(d), respectively. The maximum modeling errors of Fig. 8 are about 8.8% of the amplitude of the input (or 3.2 μm). It indicates that the proposed T-S fuzzy modeling is acceptable.

C. Control Performance

The switching surface (12) for the proposed control is selected as follows: $\sigma(k) = e(k) - 0.4e(k-1) + 0.18e(k-2) + 0.04e(k-3)$, they are in well-damped region [13]. The fuzzy switching control $u_{sw}^i(k)$ [or $v_{sw}^i(k)$] uses the following control parameters: $\overline{\lambda}^i = 0.02$, $\lambda_0^i = 0.001$, $\lambda_1^i = 0.01$, $\varepsilon^i = 0.3$, $\xi^i(k) = \xi_1^i(k) + 0.9g_1^i(k)\{1 - 0.98e^{-1000|\sigma(k)|}\}$, and $\beta^i(q^{-1}) = \left(1.4 - 0.6q^{-1}\right)/\left(1.6 - 0.2q^{-1}\right)$. The corresponding switching control gain [i.e., $\eta^i(q^{-1})$] is a low-pass filter attenuating the high-frequency component of the switching control. The output of the proposed control without using the fuzzy switching control for the reference inputs: $6\sin(10\pi k) + 30\sin(20\pi k)$ μm, $36\sin(30\pi k)\mu m$, $36\sin(10\pi k)$ μm, and $36\sin(20\pi k)$ μm, are shown in Fig. 9(a)–(d), respectively. The maximum steady-state tracking errors of Fig. 9 are about 8.9% (cf. Table I). The control performance is dependent on the accuracy of the T–S fuzzy model.

The output response of the proposed control for the same reference inputs of Fig. 9 are presented in Fig. 10(a)–(d), respectively. Their maximum steady-state tracking errors are about 4.5% of the magnitude of the corresponding reference input (cf. Table I). The maximum steady-state tracking errors of Figs. 9 and 10 are 8.9% and 4.5%, respectively, i.e., the fuzzy switching control improves the system performance by about 50%. The main reason for this is that the response of traditional fuzzy linear feedback control is a little inferior for the PEA system with notable hysteresis. Fig. 11(a) shows the corresponding control input of Fig. 10(a); it can be seen that the control input is

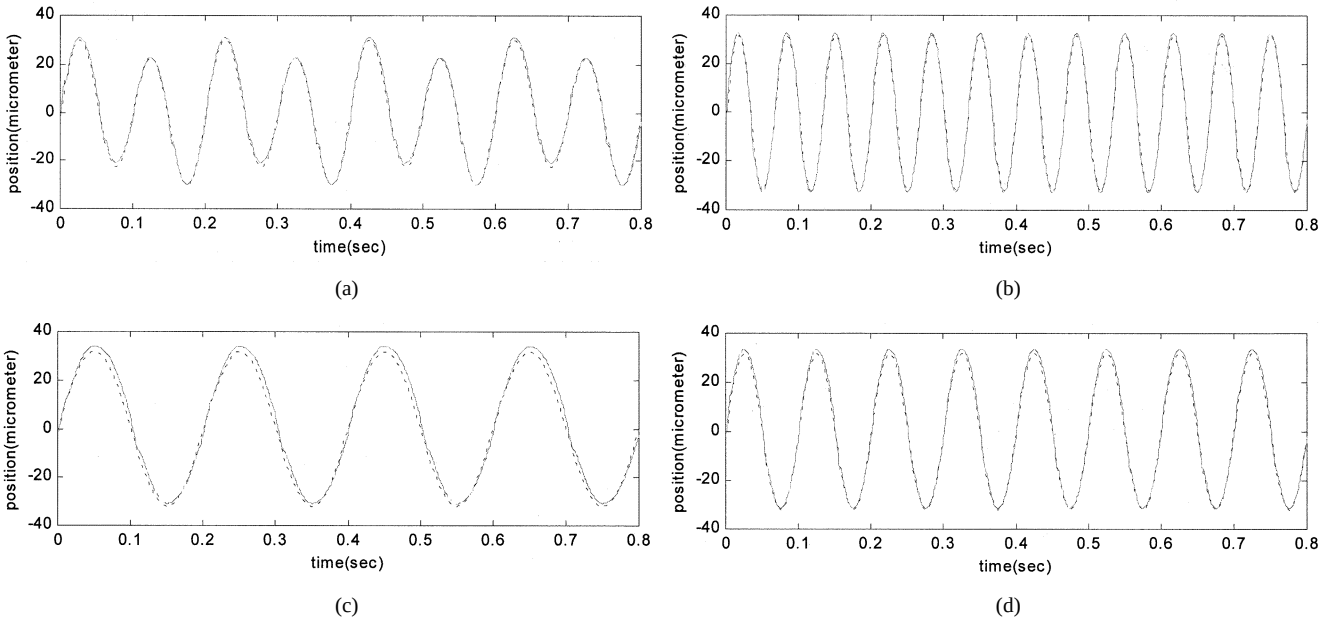

Fig. 8. The output responses of the mathematical model $(-)$ and the system $(\cdots)$ for the inputs. (a) $6\sin(10\pi k) + 30\sin(20\pi k)$ μm. (b) $36\sin(30\pi k)$ μm. (c) $36\sin(10\pi k)$ μm. (d) $36\sin(20\pi k)$ μm.

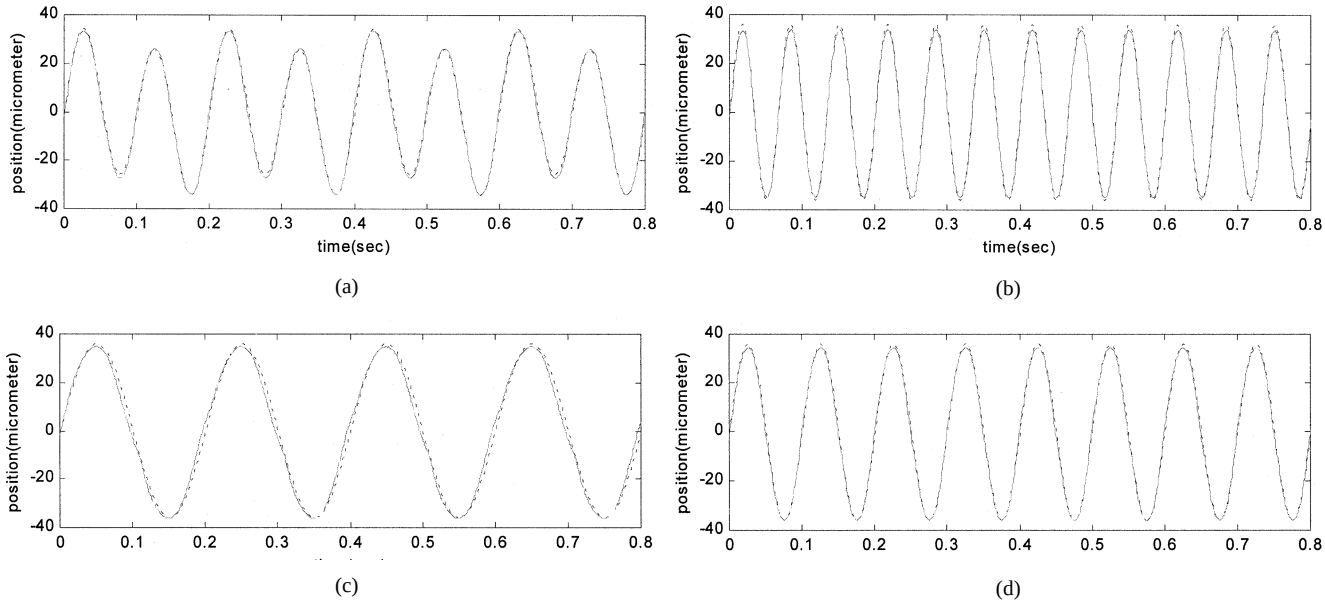

Fig. 9. The output responses of the proposed control without fuzzy switching control $(-)$ for the reference inputs $(\cdots)$. (a) $6\sin(10\pi k) + 30\sin(20\pi k)$ μm. (b) $36\sin(30\pi k)$ μm. (c) $36\sin(10\pi k)$ μm. (d) $36\sin(20\pi k)$ μm.

smooth enough. The corresponding response of the switching surface of Fig. 10(a) is shown in Fig. 11(b) that is in the neighborhood of the switching surface due to the existence of uncertainties. Although the fuzzy model (52) is identified by the combination of sinusoidal signals, the proposed controller based on this fuzzy model can be applied to track the sinusoidal trajectory of different frequencies (e.g., 5, 10, and 15 Hz). Due to the robustness of the proposed control, the tracking results are satisfactory.

VII. Conclusion

Because the dynamics of the PEA system is strongly dependent on the hysteretic behavior, the dominant factors of the hysteretic loop are the amplitude and polarity of the input signal. The frequency of the input signal only mildly affects the dynamics of the PEA. Hence, the premise variables of the T-S fuzzy linear model are selected as $u(k-1)$ and $\Delta u(k-1) = u(k-1) - u(k-2)$. After the verification of fuzzy model, the fuzzy equivalent and the fuzzy switching control are em-

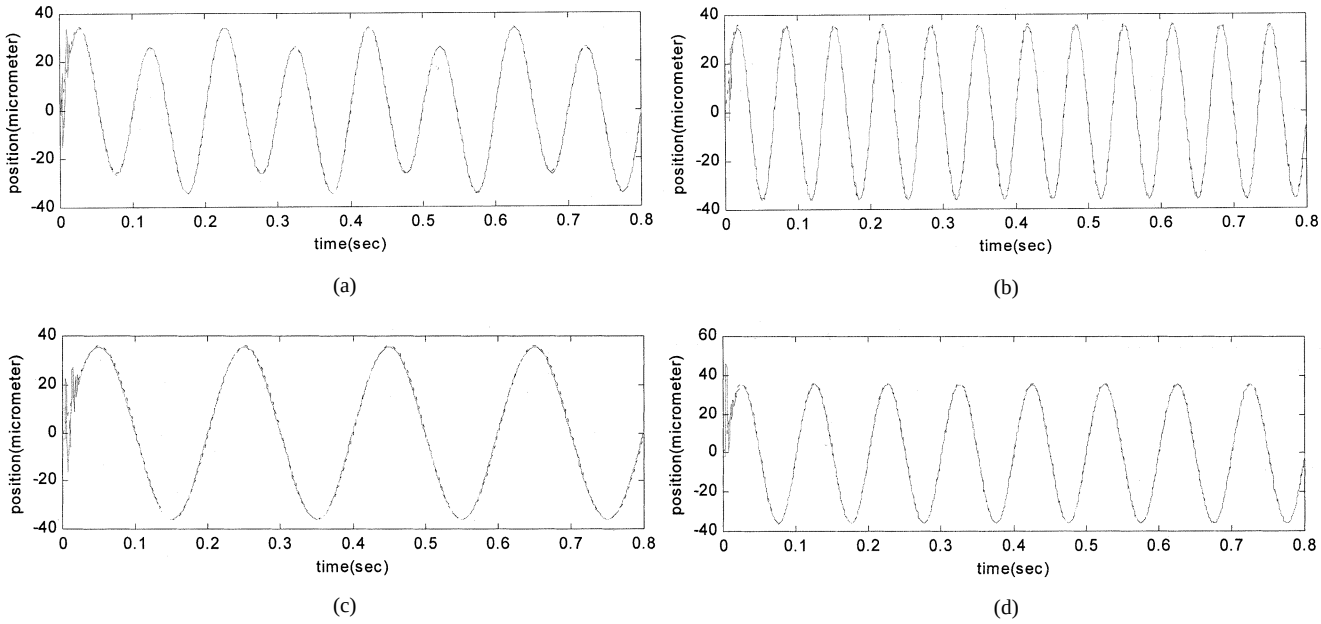

Fig. 10. The output responses of the proposed control $(-)$ for the reference inputs $(\cdots)$. (a) $6\sin(10\pi k) + 30\sin(20\pi k)$ μm. (b) $36\sin(30\pi k)$ μm. (c) $36\sin(10\pi k)$ μm. (d) $36\sin(20\pi k)\mu$m.

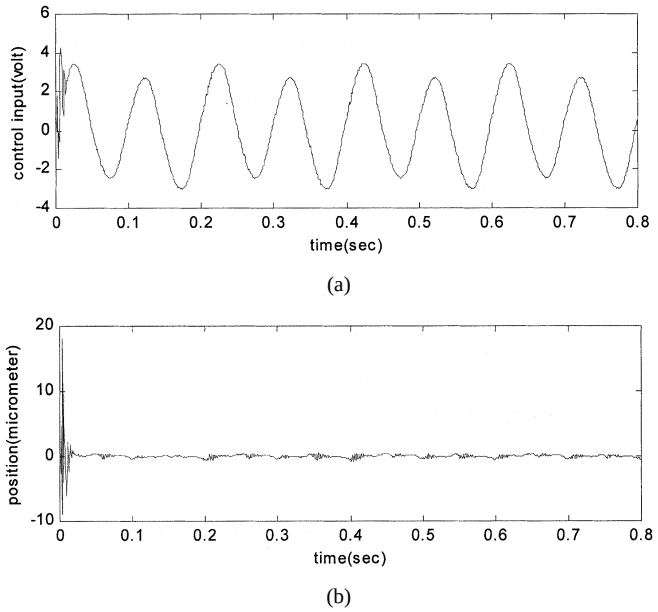

Fig. 11. The responses of the proposed control for the reference input $6\sin(10\pi k) + 30\sin(20\pi k)$ μm. (a) $u(k)$. (b) $\sigma(k)$.

ployed to control the PEA system. The fuzzy equivalent control is designed based on a technique of dead-beat to the switching surface and a minimax optimization of the sensitivity function between the switching surface and the output disturbance. Furthermore, the effect of the approximation error of fuzzy-model and the interaction dynamics resulting from other subsystems is attenuated. The fuzzy switching control is also applied to reinforce the performance in the face of the approximation error and the interaction dynamics. In this situation, the performance of the proposed control is better than that of traditional fuzzy linear feedback control (e.g., the proposed control without the fuzzy switching control). In addition, the proposed control does not require a state estimator or a solution of a common positive–definite matrix for every subsystem [9]–[12]. It amalgamates the advantages of model-based fuzzy control and the robust control to accomplish an effective and simple controller for the PEA system. It is believed that it can be applied to other tracking control problems.

APPENDIX
PROOF OF THEOREM 1

The following Lyapunov function is defined:

$$V(k) = \sum_{i=1}^{N} \mu^i(k) V^i(k) = \sum_{i=1}^{N} \mu^i(k)\sigma^i(k)^2/2 > 0 \quad \text{as } \sigma^i(k) \neq 0. \tag{A1}$$

In fact, $V(k) = \sigma(k)^2/2$. Then, the change rate of (A1) is given as follows:

$$\Delta V(k) = \sum_{i=1}^{N} \mu^i(k) \left\{ V^i(k+d^i) - V^i(k) \right\} = \sum_{i=1}^{N} \mu^i(k) \left\{ \sigma^i(k)\Delta\sigma^i(k) + \Delta\sigma^i(k)^2/2 \right\}. \tag{A2}$$

First, $|\sigma(k)| > \chi^i(k)$ is considered. Suppose $\Delta V(k) \leq -\varepsilon V(k)$, where $\varepsilon = \min\left(\varepsilon^i\right), 0 < \varepsilon^i < (1-\overline{\lambda}^i)^2/(1+\overline{\lambda}^i)^2 < 1$. Then, the following equation is achieved by using (40), (43), (44), (A1), (A2), and the fact $\sigma^i(k) = \sigma(k)$

$$\Delta\overline{V}(k) = \Delta V(k) + \varepsilon V(k) \leq \sum_{i=1}^{N} \mu^i(k)\sigma(k) \left\{ \Lambda^i(k) + \left[1 - \tau^i(q^{-1}, k)\right] v_{sw}^i(k) \right\}$$

$$+\sum_{i=1}^{N}\mu^i(k)\left\{\Lambda^i(k)+\left[1-\tau^i(q^{-1},\,k)\right]v_{sw}^i(k)\right\}^2 \Bigg/ 2+\sum_{i=1}^{N}\mu^i(k)\varepsilon^i\sigma(k)^2 \Bigg/ 2$$
$$\le \sum_{i=1}^{N}\mu^i(k)\left\{|\sigma(k)|\,g_\lambda^i(k)-\frac{\xi^i(k)g_\lambda^i(k)\,|\sigma(k)|}{1+\overline{\lambda}^i}+\frac{g_\lambda^i(k)^2}{2}+\frac{\xi^i(k)g_\lambda^i(k)^2}{1-\overline{\lambda}^i}+\frac{\left[\xi^i(k)g_\lambda^i(k)\right]^2}{2(1-\overline{\lambda}^i)^2}+\frac{\varepsilon^i\sigma(k)^2}{2}\right\}$$
$$=\sum_{i=1}^{N}\mu^i(k)\left\{g_\lambda^i(k)^2 g^i(\xi^i)\,/\left[2(1-\overline{\lambda}^i)^2\right]\right\} \tag{A3}$$

where

$$g^i(\xi^i)=\xi^i(k)^2-2g_1^i(k)\xi^i(k)+g_2^i(k). \tag{A4}$$

If $g^i(\xi^i)\le 0$, for $i=1,2,\ldots,N$, then $\Delta\overline{V}(k)\le 0$ [or $\Delta V(k)\le -\varepsilon V(k)$]. Because

$$|\sigma(k)|>4(1+\overline{\lambda}^i)g_\lambda^i(k)\,/\left[(1-\overline{\lambda}^i)^2-\varepsilon^i(1+\overline{\lambda}^i)^2\right] \tag{A5}$$

both $g_1^i(k)>0$ and $g_1^i(k)^2-g_2^i(k)>0$ for $i=1,2,\ldots,N$, are achieved. Substituting (43) into (A5) yields

$$|\sigma(k)|>4(1+\overline{\lambda}^i)\lambda_1^i \Big/\left[(1-\overline{\lambda}^i)^2-\varepsilon^i(1+\overline{\lambda}^i)^2-4(1+\overline{\lambda}^i)\lambda_0^i\right]. \tag{A6}$$

From (A5) and (A6), (46) is achieved. In summary, the switching gain chosen from (47) makes $\Delta V(k)\le -\varepsilon V(k)$. Then, $\{\sigma(k),\,u(k)\}$ are bounded and the performance (48) is accomplished.

Similarly, the case $|\sigma(k)|\le\chi^i(k)$ is obtained. Q.E.D.

REFERENCES

[1] Y. Okazaki, "A micro-positioning tool post using piezoelectric actuator for diamond turning machines," *Precision Eng.*, vol. 12, no. 3, pp. 151–156, 1990.

[2] A. B. Palazzolo, S. Jagannathan, A. F. Kascak, G. T. Montague, and L. J. Kiraly, "Hybrid active vibration control of rotor bearing systems using piezoelectric actuators," *ASME J. Vibrat. Acoust.*, vol. 115, pp. 111–119, 1993.

[3] C. J. Li, H. S. M. Beigi, S. Li, and J. Liang, "Nonlinear piezo-actuator control by learning self-tuning regulator," *ASME J Dyna. Syst. Meas. Control*, vol. 115, pp. 720–723, 1993.

[4] S. B. Jung and S. W. Kim, "Improvement of scanning accuracy of PZT piezoelectric actuator by feed-forward model-reference control," *Precision Eng.*, vol. 16, no. 1, pp. 49–55, 1994.

[5] G. Tao and P. V. Kokotovic, "Adaptive control of plants with unknown hysteresis," *IEEE Trans. Automat. Contr.*, vol. 40, pp. 200–212, Feb. 1995.

[6] P. Ge and M. Jouaneh, "Tracking control of a piezoceramic actuator," *IEEE Trans. Contr. Syst. Technol.*, vol. 4, pp. 209–216, Mar. 1996.

[7] B. M. Chen, T. H. Lee, C. C. Hang, Y. Guo, and S. Weerasooriya, "An H^∞ almost disturbance decoupling robust controller design for a piezoelectric bimorph actuator with hysteresis," *IEEE Trans. Contr. Syst. Technol.*, vol. 7, pp. 160–174, Feb. 1999.

[8] C. L. Hwang, C. Jan, and Y. H. Chen, "Piezomechanics using intelligent variable structure control," *IEEE Trans. Ind. Electron.*, vol. 48, pp. 47–59, Feb. 2001.

[9] T. Takagi and M. Sugeno, "Fuzzy identification of systems and its applications to modeling and control," *IEEE Trans. Syst., Man, Cybern.*, vol. SMC-15, pp. 116–132, Feb. 1985.

[10] K. Tanaka, T. Ikeda, and H. O. Wang, "Robust stabilization of a class of uncertain nonlinear systems via fuzzy control: Quadratic stabilizability, H^∞ control theory, and linear matrix inequality," *IEEE Trans. Fuzzy Syst.*, vol. 4, pp. 1–13, Feb. 1996.

[11] B. S. Chen, C. S. Tsen, and H. J. Uang, "Robustness design of nonlinear dynamic systems via fuzzy linear control," *IEEE Trans. Fuzzy Syst.*, vol. 7, pp. 571–585, Oct. 1999.

[12] T. A. Johansen, R. Shorten, and R. Murray-Smith, "On the interpretation and identification of dynamic Takagi–Sugeno fuzzy models," *IEEE Trans. Fuzzy Syst.*, vol. 8, pp. 297–313, June 2000.

[13] K. J. Åström and B. Wittenmark, *Computer-Controlled Systems—Theory and Design*, 3rd ed. Upper Saddle River, NJ: Prentice-Hall, 1997.

[14] M. Vidyasagar, *Control System Synthesis—A Factorization Approach.* Cambridge, MA: MIT Press, 1985.

[15] C. L. Hwang, "A fuzzy-linear-model-based variable structure control for nonlinear discrete-time systems," in *Proc. IEEE Int. Conf. Industrial Electronics, Control Instrumentation*, Nagoya, Japan, Oct. 22–28, 2000, pp. 536–541.

[16] B. A. Francis, *A Course in H_∞ Control Theory*. Berlin, Germany: Springer-Verlag, 1987, Lecture Notes in Control and Information Sciences.

[17] C. L. Hwang and B. S. Chen, "Adaptive control of optimal model matching in H^∞-norm space," in *Proc. Inst. Elect. Eng. D—Control Theory Applications*, vol. 135, 1988, pp. 295–301.

[18] C. L. Hwang, "Robust discrete variable structure control with finite-time approach to switching surface," *Automatica*, vol. 38, no. 1, pp. 167–175, 2002.

Chih-Lyang Hwang received the B.E. degree in aeronautical engineering from Tamkang University, Taiwan, R.O.C., and the M.E. and Ph.D. degree in mechanical engineering from Tatung Institute of Technology, Taiwan, R.O.C., in 1981, 1986, and 1990, respectively.

Since 1990, he has been with the Department of Mechanical Engineering of Tatung Institute of Technology, where he is currently engaged in teaching and research in the area of servo control and control of manufacturing systems as a Professor of Mechanical Engineering. In 1998–1999, he was a Research Scholar at the George W. Woodruff School of Mechanical Engineering, Georgia Institute of Technology, Atlanta. He is the author or coauthor of approximately 70 journal and conference papers in related fields. His current research interests include fuzzy (neural-network) modeling and control, variable structure control, mechatronics, robotics, visual servosystem, and Internet-based control.

Dr. Hwang was a Technical Committee Member of IEEE IECON02. He has received a number of awards, including the Excellent Research Paper Award from the National Science Council of Taiwan and Hsieh-Chih Industry Renaissance Association of Tatung Company.

Chau Jan was born in Taiwan, R.O.C., in 1972. He received the B.E. degree from the Department of Mechanical Engineering, National Cheng Kung University, Tainan, Taiwan, R.O.C., and the M.E. degree from Tatung University, Taipei, Taiwan, R.O.C., in 1996 and 1998, respectively, both in mechanical engineering. He is currently working toward the Ph.D. degree in mechanical engineering at Tatung University.

His current research interests include control system, robust control, neural networks, fuzzy logic theory, piezomechanics, and dynamic systems.